Published in final edited form as:
*Cancer Res*. 2008 December 1; 68(23): 9935–9944. doi:10.1158/0008-5472.CAN-08-2139.

# Chromosome 12p deletions in *TEL-AML1* childhood acute lymphoblastic leukemia are associated with retrotransposon elements and occur postnatally

**Joseph L. Wiemels**[1], **Jerry Hofmann**[1], **Michelle Kang**[1], **Rebecca Selzer**[2], **Roland Green**[2], **Mi Zhou**[1], **Sheng Zhong**[1], **Luoping Zhang**[3], **Martyn T. Smith**[3], **Carmen Marsit**[4], **Mignon Loh**[5], **Patricia Buffler**[6], and **Ru-Fang Yeh**[1]

1*Laboratory for Molecular Epidemiology, Department of Epidemiology and Biostatistics, UCSF*

2*Roche Nimblegen Systems*

3*Division of Environmental Health Sciences, School of Public Health, University of California at Berkeley*

6*Division of Epidemiology, School of Public Health, University of California at Berkeley*

4*Department of Pathology and Laboratory Medicine, Brown University, Providence RI*

5*Department of Pediatrics, UCSF*

## Abstract

*TEL-AML1 (ETV6-RUNX1)* is the most common translocation in the childhood leukemias, and is a prenatal mutation in most children. This translocation has been detected at a high rate among newborns (~1%); therefore the rate-limiting event for leukemia appears to be secondary mutations. A frequent such mutation in this subtype is partial deletion of chromosome 12p, *trans* from the translocation. Nine del(12p) breakpoints within six leukemia cases were sequenced to explore the etiology of this genetic event, and most involved cryptic sterile translocations. Twelve of 18 del(12p) parent sequences involved in these breakpoints were located in repeat regions (8 of these in Long Interspersed Nuclear Elements, or LINEs). This stands in contrast to *TEL-AML1*, in which only 21 of 110 previously assessed breakpoints (19%) occur in DNA repeats ($P = 0.0001$). An exploratory assessment of archived neonatal blood cards (ANB cards) revealed significantly more LINE CpG methylation in individuals at birth who were later diagnosed with *TEL-AML1* leukemia, compared to individuals who did not contract leukemia ($P = 0.01$). Nontemplate nucleotides were also more frequent in del(12p) than in *TEL-AML1* junctions ($P = 0.004$) suggesting formation by terminal deoxynucleotidyl transferase. Assessment of six ANB cards indicated that no del(12p) rearrangements backtracked to birth, although two of these patients were previously positive for *TEL-AML1* using the same assay with comparable sensitivity. These data are compatible with the a two-stage natural history: *TEL-AML1* occurs prenatally, and del(12p) occurs postnatally in more mature cells with a structure that suggests the involvement of retrotransposon instability.

Correspondence to: Joseph L. Wiemels.

Address reprint requests to Joseph Wiemels, UCSF Box 0441, 1 Irving Street, AC-34, San Francisco CA 941143-0441..

**Contributions of authors**: J.W. designed the study, performed some of the lab work, and drafted the manuscript. J.H and M.K. performed most of the laboratory work and constructed some of the figures and tables, and contributed to the drafting of the manuscript. R.S. and R.G. performed the array comparative genomic hybridizations and contributed to statistical analysis. M.S. and S.Z. and C.M. performed retrotransposon methylation assays and contributed to manuscript preparation. L.Z and M.T.S. performed FISH classification studies, karyotype reviews, and initial sample processing. P.B. and M.L. designed the NCCLS study and the sample repository and contributed to the scientific analysis, biomaterials, and manuscript preparation. R-F.Y. performed statistical analysis, constructed figures, and contributed to scientific analysis and manuscript write-up.

**Keywords**

childhood acute lymphoblastic leukemia; etiology of chromosomal deletion; retrotransposon; Guthrie card; backtracking

## Introduction

Acute lymphoblastic leukemia is the most common diagnosis in childhood cancer; and about 22% of children harbor the t(12;21) *TEL-AML1* (*ETV6-RUNX1*) translocation. We and others have found that the *TEL-AML1* translocation associated with pediatric leukemia often occurs before birth - a total of 36 patients along with their paired archived neonatal blood spots (ANB cards) have been tested with 18 ANB cards demonstrating the fusion gene (50 %) (1-4). Twin studies have also shown that concordant leukemias in identical twins are often a result of an *in utero TEL-AML1* translocation that spread from one twin to the other (5-8), which led Greaves and colleagues to propose a two stage model for this leukemia beginning with the translocation before birth. Strikingly, the *TEL-AML1* translocation was shown to be quite prevalent among newborns (~1%) (9). This revealed that the t(12;21) translocation was not sufficient for leukemia and that complementary and subsequent mutations are the rate limiting event.

Along with the translocation, approximately 70% of *TEL-AML1*$^+$ leukemias exhibit a loss of the *other* chromosome 12 (the allele not involved in the translocation). The del(12p) is the most common complementary event, and is likely secondary since it is subclonal to the translocation in some patients (10). More evidence that the del(12p) is secondary to t(12;21) is the variable del(12p) endpoints among patients with the same *TEL-AML1* translocation at both initial diagnosis and relapse (11,12). Elucidating the timing and mechanism of this rearrangement may contribute to preventive measures for leukemia. A variety of other genetic rearrangements have been recently identified as complementary events to *TEL-AML1* using high density SNP arrays including *INK4A/B* and *PAX5*, but each with a much lower prevalence than del(12p) (13).

Extensive microsatellite mapping of *TEL-AML1*$^+$/del(12p) patients (14-16), as well as recent investigations utilizing high density whole genome SNP arrays (13,17,18), have supported the idea that *TEL* is the gene target of the del(12p). TEL has a dimerization domain which is retained in the TEL-AML1 chimeric protein. Both this dimerization domain and the AML1 DNA binding domain are required for oncogenesis by TEL-AML1 (19-21). The TEL protein can bind and inhibit TEL-AML1, and TEL loss in the presence of del(12p) permits the full oncogenic phenotype.

While the timing and the structure of *TEL-AML1* breakpoints are well characterized, the corresponding breakpoints of the del(12p) have not been described. These breakpoints may occur by an alternate mechanism given that they may take place after birth in a more differentiated cell. It is also possible that the 12p deletions precede the translocation in some patients. Since *TEL-AML1*+ leukemia is characterized by recombinase activating gene activity as exhibited by *RAG* expression and recurrent rearrangements at *Ig* and *TCR* loci (22-25), we hypothesized that such activity might be responsible for secondary rearrangements. The *TEL-AML1* translocations themselves display characteristics of random breakage events, *eg*., DNA breakpoints are unclustered and do not obviously associate with features such as V(D)J recombinase site sequences (RSS) or topoisomerase II sites. These observations led us to presume that such rearrangements may occur in earlier precursors than the *RAG*+ pre-B cells which present with the leukemia (26,27). In animal models TEL-AML1 activity results in an expanded precursor pool with some impedance of differentiation (28,29). We now report on

both the structure and the timing of origin of del(12p) in *TEL-AML1*+ leukemia, using a series of leukemias and their corresponding archived neonatal blood cards (ANB or Guthrie cards).

## Materials and Methods

### Study subjects

Patient samples were obtained by the Northern California Childhood Leukemia Study (NCCLS), an epidemiology study focusing on the etiology of childhood leukemia in a 35 county area of Northern and Central California. All work was performed under IRB approval, and parents provided consent for use of both diagnostic DNA samples and neonatal Guthrie cards specimens. Patient samples were subjected to a cytogenetic classification protocol as previously described (30). DNA was extracted from all ten patients by SDS/proteinase K/ phenol/chloroform methods as described, and patients were assessed for *TEL-AML1* translocation using long distance (LD) and long distance inverse (LDI) PCR (3).

### Microarray Analysis

A highly dense custom microarray, permitting sub-kilobase resolution, was used to characterize and isolate the deletion endpoints. Isothermal probes varying in length and averaging 50 bp were tiled on a maskless array synthesized microarray using photo-deprotection methods (Nimblegen Systems, Inc.). 390,000 probes were tiled along the 38 megabase *p* arm of chromosome 12. Leukemia DNA labeled with Cy3 and normal control peripheral blood DNA (consisting of expired blood donor-derived DNA) labeled with Cy5 were competitively hybridized to the microarray. Arrays were scanned with an Agilent two-color scanner.

Probe intensities were extracted from images of hybridized arrays using NimbleScan 2.0 software, and quantile-normalized to remove systematic biases. The sample to reference probe intensity ratios (in logarithm base 2) were averaged within nonoverlapping 5kb windows, and regions of estimated equal copy number were derived using a circular binary segmentation algorithm implemented in the DNAcopy package from R/bioconductor: www.bioconductor.org. In addition, lowess lines were constructed at increasing zoom levels to estimate the breakpoints at a sub-kilobase resolution to permit attempts at sequencing breakpoints. All genome location information is based on Human Genome Release 18.

### Sequencing and Backtracking

Chromosome 12p deletions were sequenced at the nucleotide level using both LD- and LDI-PCR. Sequencing of interstitial deletions, meaning a portion of the 12p arm was lost but both the telomere and centromere retained, was first attempted with LD-PCR. Pairs of primers were synthesized at the two margins of the breakpoint, leading to nested LD-PCR with the PCR buffer and cycling conditions as described (31). In other cases where the distal portion of chromosome 12p was lost (inclusive of the telomere) with only a single breakpoint evident, LDI-PCR was attempted. In this case two pairs of primers were located in opposing directions anchored to the side of the breakpoint. As noted in Results, nested PCR was used to both increase specificity (by using two sets of primers) and increase the amount of PCR product for sequencing. A more complete description of these sequencing methods is described earlier (32).

Backtracking of del(12p) breakpoints was performed using a two step nested PCR for maximal sensitivity (PCR primers in Supplementary Table S1). This two-round PCR was first determined to detect single DNA copies of translocation events using mock ANB cards spiked with cell line cells, which harbor a specific translocation. DNA was isolated from ANB cards using the blood spot protocol of the Qiagen DNA Micro kit. About 250 ng of DNA was isolated from each 1/8 segment of a 1.5 $cm^2$ ANB card; 50 ng or approximately 8300 cell equivalents,

was used in repeat PCRs. Sensitivity was established with each PCR assay using a dilution series of patient DNA. Appropriate precautions, including the use of positive displacement pipettes, separate laboratory areas for DNA isolation, first and second round PCR set-up, and use of multiple controls were instituted during ANB card backtracking.

### LINE methylation analysis

A Taqman LINE methyation assay was used as previously described by Weisenberger *et al.* with some modification (33). Alu C4 was used as the DNA input control, and an assay targeting the bisulfite product of methylated LINE-M1 sequence was used as the test reaction. DNA was isolated from 51 ANB card DNA samples, 35 derived from children who contracted leukemia (10 *TEL-AML1*+, and 25 non-*TEL-AML1* cALL) and 19 frequency-matched by age, race, and ethnicity to the case ANB cards. All cards were provided by the California Genetic Diseases Branch (Department of Health Services) at the same time and were processed and stored under identical conditions. Guthrie card DNA samples were coded and randomized prior to analysis. One ug DNA (Qiagen Micro kit, blood card protocol) was treated with bisulfite (Zymo Research). WGA DNA and "CpGenome" universal methylated DNA (Zymo) were treated with the same reagent and method and used as the negative and positive control of the methylation assay, respectively. A plasmid containing target sequence for the LINE1-M1 and Alu C4 Taqman reactions was used at the concentrations of 5.0ng/uL, 0.5 ng/uL, 0.05 ng/uL, 0.005 ng/uL, 5E-4 ng/uL, 5E-5 ng/uL, 5E-6 ng/uL, 5E-7 ng/uL to set up standard curves. Primers and probes are listed in Supplementary Table 1. In a 10 ul reaction, 1 ul of plasmid standard or treated ANB card DNA (10 ng measured pre-bisulfite treatment) DNA was run with 3.5 pM each primer, 1 pM probe, TaqMan master mix, in an ABI 7900 HT PCR machine: 95°C for 10 minutes, 50 cycles at 95°C for 15 seconds, 53°C for 1 minute. All DNA samples were run in duplicate on a 384-well plate. The results are shown as pre-calculated mean quantity (Mean Qty) for the duplicate sample data. Percent Methylated Reference (PMR) of each sample was calculated using the following equation: PMR=((Mean Qty of sample using LINE1-M1 primers)/(Mean Qty of sample using AluC4 primers))/((Mean Qty of universal methylated DNA sample using LINE1-M1 primers)/(Mean Qty of universal methylated DNA sample using AluC4 primers))X100.

### Breakpoint Motif Analysis

Statistical analysis of DNA breakpoints was performed using custom scripts commands in the statistics environment *R*. Repeats were determined by RepeatMasker (version 3.1.3, Feb 2006 version). Differences between *TEL-AML1* and del(12p) breakpoints with regard to proximity to repeats was determined using Fisher's exact test. Statistical analysis of proximity of various features (searched using EMBOSS/Fuzznuc or custom perl scripts) including repeat regions (such as SINE, LINE, LTR, transposon fossils, and simple repeats), putative matrix attachment regions (34), topoisomerase II sites (35), and pyrimidine tracts (36), was performed by comparing the observed proximity of breakpoints to these features to 200 random simulations of the dispersal of breakpoints and the features within the space of the target *TEL* and *AML1* introns. This analysis was not possible for the 12p deletions that occur on a much larger and variable scale. LINE methylation data were logarithm (base 10) transformed and analyzed using Student's T-Test and ANOVA, and box and whisker plots were used for visualization.

## Results

Seven of ten patients in this study presented with a "normal" 46 chromosome Giemsabanding karyotype. Patient #5 had 46 chromosomes in 8/9 mitoses, and 45 (lacking chromosome 20) in 1/9 mitoses. Karyotype analysis failed in patients #3 and #7, due to lack of cell growth. All patients demonstrated *TEL-AML1* translocation by FISH using conventional probes (Vysis), and 9 of 10 had a deletion of the second *TEL* allele in the same FISH analysis.

In order to track and sequence large-scale deletions, identification of breakpoints requires kilobase-level precision rather than the hundred-kilobase resolution common with most CGH methods. This proved to be feasible using a microarray method (37) which we used to tile long isothermal oligonucleotides along the 38 megabase *p* arm of chromosome 12 (37). Four of the ten breakpoints showed apparent interstitial deletions (patients 1, 3, 4 and 5). Five demonstrated single breakpoints with the deletion of the remainder of the chromosome arm (Figure 1A). A single patient who did not harbor a 12p deletion by FISH using a *TEL* probe (Vysis) (Patient #6) did not harbor any copy number changes in 12p. The patient with the lowest proportion of del(12p)-positive TEL-AML1 cells in FISH assays [patient #2: 70% of TEL-AML1 cells had del(12p)] also displayed the weakest copy number loss "$Log_2$ ratio" (Figure 1). For this and the other eight samples, we believe the del(12p) shown is the dominant leukemic clone. The smallest "commonly deleted region" was defined by patients 3 and 4, centromeric and telomeric side, respectively. This region was bounded at position 11,918 kB and 13,119 kB and contained 11 genes, including the telomeric half of *TEL* (exons 6-8, see Figure 1B). Using the high density probe design, zoomed views of the apparent breakpoints allowed for sub-kilobase resolution of breakpoints in some cases, or at least estimations within 10 kb (Figure 2). Several common copy number polymorphisms were also evident in the array-CGH such as a deletion polymorphism at approximately 32 MB position, which was evident in patients #1, 3, 5, 7, 8, and 9. Note that a common normal reference DNA was used in the array-CGHs for all patients, not individually matched constitutive DNAs.

Following the fine mapping of breakpoints, we used LD- or LDI-PCR to sequence fusion junctions. We utilized nested PCR for two reasons: to increase specificity of PCR reactions, and to increase the amount of PCR product for sequencing purposes. Despite the appearance of interstitial deletions for four patients on the microarray, only two could be sequenced using conventional LD-PCR across the deletion (#5 and 8). Patient #5 had a clean deletion with no intervening sequence (Figure 2A). Patient #8 did not have a simple interstitial deletion but rather a portion of chromosome 5 and an inverted portion of chromosome 12 obtained within the PCR product anchored by primers surrounding the interstitial deletion.

When patients exhibited terminal deletions on the microarray (#2, 7, 8, 9, and 10; Figure 1), we assumed that some non-chromosome 12 sequence, or telomere, would "cap" the shortened chromosome. We used PCR methodology that would detect either of these options, but found that in all cases a sequence from another chromosome was involved. Chromosomes 2, 4, 5, 9, 12, 13, and 19 were involved in breakpoints for various patients (Table 1). While in many cases retrotransposon sequences were found at or near fusions, in all cases we were able to make high quality BLAST matches to these partner chromosomes by fully sequencing inverse PCR products. In no case were these translocations predicted to form an in-frame fusion gene or the aberrant juxtaposition of a promoter region to another gene (Table 1). None of these translocations involved the *TEL* gene, and all were confirmed using independent PCR reactions, with appropriate controls to confirm that they are specific to the leukemic clone. There were no recurrent patterns to the translocation breakpoints, and karyotypic analysis did not indicate any balanced translocations. Fine mapping of the breakpoints indicated that 2 breakpoints contained microhomologies (22%), and 5 contained nontemplate (*N*) nucleotides (56%, Supplementary Figure S1). Two other breakpoints, both from patient #8, were clean blunt-ended fusions (Supplementary Figure S1). Attempts at sequencing breakpoints in patients #3, 4, and 7 were not successful. In the case of patient #4 the attempt to clone del(12p) resulted in sequencing the *TEL-AML1* translocation and its reciprocal (data not shown).

Backtracking of patient breakpoints was performed using similar methodology as backtracking of the translocations in previous reports, with similar levels of sensitivity (3,4). Two breakpoints were analyzed for two patients, and one for the remaining four patients (Table 1). Patient #8 exhibited a "weak" band on an electrophoretic gel after the second round of PCR

that was not the correct sequence of the breakpoint fusion. A second PCR did not yield this band. In addition, a second deletion junction from this patient was also tested by Guthrie card PCR and yielded no band. We classified this patient with the others as "negative" for the presence of del(12p) at birth. In contrast to *TEL-AML1* translocation, del(12p) did not backtrack to birth in any patients. Results for some backtracking assays are displayed in Figure 3.

The del(12p) rearrangements were highly associated with interspersed repeat regions when compared to *TEL-AML1* translocations ($P = 0.00009$, Supplementary Table S2, S3, and Figure 4). This association disappeared when the window of inquiry around the breakpoint was increased to 500 base pairs ($P = 0.7$, Supplementary Table S3), suggesting that there is not an overall difference in retrotransposon sequence in the vicinity of *TEL-AML1* fusion breakpoints compared to del(12p) breakpoints. The *TEL* and *AML1* introns do have fewer DNA repeats (28% and 23%, respectively) when compared to the genome (45%). However, there was no association with these intronic repeat regions in the *TEL* and *AML1* introns at any higher frequency than would be expected at random (P = 0.7). In addition, *TEL* and *AML1* breakpoints were not associated with other specific features thought to be involved in some translocations, including scaffold attachment regions, mammalian topoisomerase II sites, and polypyrimidine tracts (data not shown). In addition to this, scanning of *TEL-AML1* and del(12p) breakpoints for heptamer-nonamer recombination site sequences (38) yielded no matches to patient breakpoints (data not shown).

To explore whether a defect of a constitutive methylation of retrotransposon elements might contribute to instability and del(12p), we used a real-time "Methylight" assay to quantify methylation status at LINE-M1 elements. There are over 200 LINE elements in this family scattered around the genome and chromosome 12 has an average prevalence of these elements. This assay was chosen since it has a high correlation with global DNA methyl-cytosine content [measured by HPLC(33)] which reflects the presence of methyl groups on cytosines on repetitive DNA elements such as retrotransposon fossils. ANB card DNA from *TEL-AML1* patients harbored significantly higher methylation status than ANB card DNA derived from children who did not contract leukemia (P = 0.01, Student's t-test, see Figure 5). Common ALL patients (CD19+, CD10+) that did not have *TEL-AML1* also had a higher median value of LINE1-M1 methylation but when compared with control children, did not reach statistical significance (P = 0.052, t-test).

## Discussion

Among the common childhood acute leukemias, those with *TEL-AML1* translocations are the best characterized in terms of the natural history of leukemogenic events. In this report we explore the timing and structure of a proposed "secondary" event - deletion of the *p* arm of chromosome 12. We have found no evidence for prenatal origin of del(12p) breakpoints. Despite the small number of patient samples tested here, the result marks a strong contrast to the *TEL-AML1* translocation, which we have found to be prenatal in 14/24 cases tested (58%) (3,4). Two of these patients who previously demonstrated prenatal *TEL-AML1* did not have the presence of the del(12p) at birth (at similar sensitivity levels); therefore, our results are quite consistent with the proposed two-hit model for this subtype of leukemia (4,12).

*TEL-AML1*$^+$ leukemia is characterized by a pre-B cell phenotype and high activity of recombinase activating gene components as exemplified by the continuous rearrangements of *IGH*, *IGK*, *IGL*, as well as ectopic rearrangements of *TCR* loci (23-25). Despite this, we and others have found no evidence for a causal role of RAG activity in *TEL-AML1* translocations. Such evidence would consist of recombinase site sequences, *N*-nucleotides, or other features commonly seen with *RAG*-associated fusions in the lymphoid neoplasms (26,27,39). The translocation may occur prior to the activation of RAG and TdT. As the rate-limiting event in

leukemia with *TEL-AML1*, we hypothesized that the del(12p) might take place in an ontologically similar cell type as presents with the diagnosis of leukemia and may be caused by RAG activity. In support of this, the del(12p) breakpoints displayed the presence of nontemplate nucleotides at most breakpoints (5 of 9) although this is a rare feature of *TEL-AML1* translocations (only 5 of 53, 9%; P = 0.004 for the difference, Fisher's exact test). This would suggest formation of del(12p) at a time when terminal deoxynucleotidyl transferase was active. The breakpoints did not, however, coincide with recombination site sequences, which are a feature of RAG-mediated recombination. This does not entirely rule out RAG involvement, as structural features including the propensity to form singlestrand or hairpin structures are known targets of RAG activity. Such structures can form within retrotransposon sequences (41,42).

The robust presence of interspersed repeat regions (particularly LINE and SINE) at the del (12p) breakpoints (Figure 4 and Supplementary Tables S2, S3) suggests two possibilities - first, that homologous recombination of such sequences was responsible for the repair of DNA breaks, or that these sequences are inherently more prone to DNA breaks. The first of these mechanisms is ruled out since none of the breakpoint fusions are products of homologous recombination. Instead, breakpoints display features of nonhomologous end-joining (NHEJ). Features of NHEJ junctions include lack of extensive homology at breakpoints or the presence of 1-8 base pair microhomologies. Microhomology is present at 2 del(12p) breakpoints, and blunt-end joining in all the remainder. Instead, retrotransposons may be more prone to breakage than the rest of the genome. Transposon-derived repeats make up close to 46% of the genome (43). These sequences are heavily methylated and repressed in normal somatic tissues (44) though they are often aberrantly hypomethylated in cancer (45). It is recognized that global hypomethylation of the genome is a common and possibly early event in carcinogenesis, and demethylation leads to chromosome instability in a mouse model (46). In relation to the proposed natural history of childhood leukemia presented here, activation and maturation of B-cells during an infection (leading to high levels of cell division and methyl-group requirements) may lead to the hypomethylation of LINE and SINE elements, DNA instability, and chromosome breaks. Ectopic expression of LINE open reading frames by demethylation in cell cultures has been demonstrated to cause multiple double strand breaks (48,49). Such breaks, if aberrantly repaired by NHEJ mechanisms, could result in the type of rearrangements seen in the del(12p) rearrangements seen here. To explore further, we utilized a previously validated assay of global LINE methylation status with the hypothesis that children with lower methylation in LINE elements may be predisposed to del(12p) and leukemia. Remarkably, we found a significant association in the reverse direction: children with *TEL-AML1*+ leukemia are born with higher LINE1-M1 methylation than children who do not contract leukemia (see Results and Fig. 5). This result, while exploratory and needing confirmation, suggests that methylation of LINE is deregulated in these individuals, or that the heavier methylation status is a reflection of prior or continuous ectopic activation of LINE elements leading to heavier methylation status. Younger and active LINE elements are known to be more heavily methylated than older LINE fossils that have mutated due to genetic drift (50); heavier methylation of LINE elements in a genome may be a reflection of more active retrotransposon activity. This result demands further investigation and serves a purpose here to identify a potential constitutive defect among children who contract leukemia with *TEL-AML1*. Since it is estimated that only 1 of 100 children born with *TEL-AML1* progress to disease (9), the LINE methylation defect indicated here is a candidate risk factor for leukemia progression, which must be be confirmed in population-based studies. To be sure, it should be noted that chromosome 12 harbors an average frequency of LINE1-M1 elements; our assay assessed genome wide methylation rather than chromosome or locus-specific methylation levels.

It should also be noted that TEL-AML1 protein targets transcriptional repression via histone deacetylase (51), a process that can precede CpG methylation (52,53). This specific promoter

methylation activity is independent of processes that lead to global DNA methylation at retrotransposons. *TEL-AML1* is a prenatal event in most leukemia cases, but the *TEL-AML1+* clone is not likely to affect the ANB card LINE methylation result since those cells represent a small minority of assayed cells on a card (less than 1%).

Our analysis of del(12p) breaks does not exclude *TEL* as the target; all patients exhibited a deletion of at least a portion of the *TEL* gene. A single individual harbored a deletion of the last 3 exons of *TEL* but this was likely a rearrangement on the *cis* chromosome (patient 4); this patients del(12p) was not sequenced. Whether any other gene within the commonly deleted region (Figure 1B) is also critical will require the analysis of additional patient samples with a similar techniques as well as gene function studies. Current microarray methods have not ruled out every gene in the region for all patients.

In sum, the sequencing and backtracking of del(12p) rearrangements has provided additional support for the Greaves “two-hit hypothesis,” which posits that this “second” or rate-limiting mutation in this type of leukemia subtype is postnatal and can arise from aberrantly strong immunostimulation that occurs during an infection proximal to the leukemia diagnosis (54). An unexpected association of these rearrangements with SINE and LINE retrotransposons in the human genome suggests that they may contribute to their formation. Finally, the data is compatible with they hypothesis that these rearrangements occur at an ontologically more mature cell than the *TEL-AML1* translocation.

## Supplementary Material

Refer to Web version on PubMed Central for supplementary material.

## Acknowledgements

The authors wish to thank the families who participated in the NCCLS and the clinical collaborators from University of California Davis Medical Center (Dr. Jonathan Ducore), University of California San Francisco (Drs. ML and Katherine Matthay), Children's Hospital of Central California (Dr. Vonda Crouse), Lucile Packard Children's Hospital (Dr. Gary Dahl), Children's Hospital Oakland (Dr. James Feusner), Kaiser Permanente Sacramento (Dr. Vincent Kiley), Kaiser Permanente Santa Clara (Drs. Carolyn Russo and Alan Wong), Kaiser Permanente San Francisco (Dr. Kenneth Leung), and Kaiser Permanente Oakland (Dr. Stacy Month). ). JLW is a Scholar in Clinical Research of the Leukemia and Lymphoma Society of America. Supported by NIH grant CA089032 (JLW), P42-ES04705 (MTS) and R01 ES09137 (PAB), the Children with Leukaemia Fund, UK (JLW, PAB), and FAMRI YCSA (to CJM).

**Grant funding**: NIH CA89032 (to JLW), P42-ES04705 (MTS) and R01 ES09137 (PAB), the Children with Leukaemia Fund, UK (JLW, PAB), and FAMRI YCSA (to CJM).

## References

1. Andersen MT, Nordentoft I, Hjalgrim LL, et al. Characterization of t(12;21) breakpoint junctions in acute lymphoblastic leukemia. Leukemia 2001;15:858–9. [PubMed: 11368451]
2. Burjanivova T, Madzo J, Muzikova K, et al. Prenatal origin of childhood AML occurs less frequently than in childhood ALL. BMC Cancer 2006;6:100. [PubMed: 16630339]
3. McHale CM, Wiemels JL, Zhang L, et al. Prenatal origin of TEL-AML1-positive acute lymphoblastic leukemia in children born in California. Genes Chromosomes Cancer 2003;37:36–43. [PubMed: 12661004]
4. Wiemels JL, Cazzaniga G, Daniotti M, et al. Prenatal origin of acute lymphoblastic leukaemia in children. Lancet 1999;354:1499–503. [PubMed: 10551495]
5. Wiemels JL, Ford AM, Van Wering ER, Postma A, Greaves M. Protracted and variable latency of acute lymphoblastic leukemia after TEL-AML1 gene fusion in utero. Blood 1999;94:1057–62. [PubMed: 10419898]

6. Ford AM, Bennett CA, Price CM, Bruin MC, Van Wering ER, Greaves M. Fetal origins of the TEL-AML1 fusion gene in identical twins with leukemia. Proceedings of the National Academy of Sciences of the United States of America 1998;95:4584–8. [PubMed: 9539781]
7. Maia AT, Ford AM, Jalali GR, et al. Molecular tracking of leukemogenesis in a triplet pregnancy. Blood 2001;98:478–82. [PubMed: 11435320]
8. Greaves MF, Maia AT, Wiemels JL, Ford AM. Leukemia in twins: lessons in natural history. Blood 2003;102:2321–33. [PubMed: 12791663]
9. Mori H, Colman SM, Xiao Z, et al. Chromosome translocations and covert leukemic clones are generated during normal fetal development. Proc Natl Acad Sci U S A 2002;99:8242–7. [PubMed: 12048236]
10. Raynaud S, Cave H, Baens M, et al. The 12;21 translocation involving TEL and deletion of the other TEL allele: two frequently associated alterations found in childhood acute lymphoblastic leukemia. Blood 1996;87:2891–9. [PubMed: 8639909]
11. Ford AM, Fasching K, Panzer-Grumayer ER, Koenig M, Haas OA, Greaves MF. Origins of “late” relapse in childhood acute lymphoblastic leukemia with TEL-AML1 fusion genes. Blood 2001;98:558–64. [PubMed: 11468150]
12. Zuna J, Ford AM, Peham M, et al. TEL deletion analysis supports a novel view of relapse in childhood acute lymphoblastic leukemia. Clin Cancer Res 2004;10:5355–60. [PubMed: 15328172]
13. Mullighan CG, Goorha S, Radtke I, et al. Genome-wide analysis of genetic alterations in acute lymphoblastic leukaemia. Nature 2007;446:758–64. [PubMed: 17344859]
14. Aissani B, Sinnett D. Fine physical and transcript mapping of a 1.8 Mb region spanning the locus for childhood acute lymphoblastic leukemia on chromosome 12p12. 3. Gene 1999;240:297–305. [PubMed: 10580149]
bin/cas/tree/store/gene/cas_sub/browse/browse.cgi?year=1999&volume=240&issue=2&aid=12157
15. Montpetit A, Boily G, Sinnett D. A detailed transcriptional map of the chromosome 12p12 tumour suppressor locus. Eur J Hum Genet 2002;10:62–71. [PubMed: 11896457]
16. Montpetit A, Larose J, Boily G, Langlois S, Trudel N, Sinnett D. Mutational and expression analysis of the chromosome 12p candidate tumor suppressor genes in pre-B acute lymphoblastic leukemia. Leukemia 2004;18:1499–504. [PubMed: 15284860]
17. Kawamata N, Ogawa S, Zimmermann M, et al. Molecular allelokaryotyping of pediatric acute lymphoblastic leukemias by high-resolution single nucleotide polymorphism oligonucleotide genomic microarray. Blood 2008;111:776–84. [PubMed: 17890455]
18. Kuiper RP, Schoenmakers EF, van Reijmersdal SV, et al. High-resolution genomic profiling of childhood ALL reveals novel recurrent genetic lesions affecting pathways involved in lymphocyte differentiation and cell cycle progression. Leukemia 2007;21:1258–66. [PubMed: 17443227]
19. Gunji H, Waga K, Nakamura F, et al. TEL/AML1 shows dominant-negative effects over TEL as well as AML1. Biochem Biophys Res Commun 2004;322:623–30. [PubMed: 15325275]
20. Lee YJ, Kim JH, Bae S, Rho SK, Choe SY. Mechanism of transcriptional repression by TEL/RUNX1 fusion protein. Mol Cells 2004;17:217–22. [PubMed: 15179033]
21. Morrow M, Samanta A, Kioussis D, Brady HJ, Williams O. TEL-AML1 preleukemic activity requires the DNA binding domain of AML1 and the dimerization and corepressor binding domains of TEL. Oncogene 2007;26:4404–14. [PubMed: 17237815]
22. Szczepanski T, Beishuizen A, Pongers-Willemse MJ, et al. Cross-lineage T cell receptor gene rearrangements occur in more than ninety percent of childhood precursor-B acute lymphoblastic leukemias: alternative PCR targets for detection of minimal residual disease. Leukemia 1999;13:196–205. [PubMed: 10025893]
23. Pine SR, Wiemels JL, Jayabose S, Sandoval C. TEL-AML1 fusion precedes differentiation to pre-B cells in childhood acute lymphoblastic leukemia. Leuk Res 2003;27:155–64. [PubMed: 12526921]
24. Panzer-Grumayer ER, Cazzaniga G, van der Velden VH, et al. Immunogenotype changes prevail in relapses of young children with TEL-AML1-positive acute lymphoblastic leukemia and derive mainly from clonal selection. Clin Cancer Res 2005;11:7720–7. [PubMed: 16278392]
25. Peham M, Konrad M, Harbott J, Konig M, Haas OA, Panzer-Grumayer ER. Clonal variation of the immunogenotype in relapsed ETV6/RUNX1-positive acute lymphoblastic leukemia indicates

subclone formation during early stages of leukemia development. Genes Chromosomes Cancer 2004;39:156–60. [PubMed: 14695996]

26. Wiemels JL, Alexander FE, Cazzaniga G, Biondi A, Mayer SP, Greaves M. Microclustering of TEL-AML1 breakpoints in childhood acute lymphoblastic leukemia. Genes Chromo Cancer 2000;29:219–28.
27. Wiemels JL, Greaves M. Structure and possible mechanisms of TEL-AML1 gene fusions in childhood acute lymphoblastic leukemia. Cancer Research 1999;59:4075–82. [PubMed: 10463610]
28. Sabaawy HE, Azuma M, Embree LJ, Tsai HJ, Starost MF, Hickstein DD. TEL-AML1 transgenic zebrafish model of precursor B cell acute lymphoblastic leukemia. Proc Natl Acad Sci U S A 2006;103:15166–71. [PubMed: 17015828]
29. Tsuzuki S, Seto M, Greaves M, Enver T. Modeling first-hit functions of the t(12;21) TEL-AML1 translocation in mice. Proc Natl Acad Sci U S A 2004;101:8443–8. [PubMed: 15155899]
30. Aldrich MC, Zhang L, Wiemels JL, et al. Cytogenetics of Hispanic and White children with acute lymphoblastic leukemia in California. Cancer Epidemiol Biomarkers Prev 2006;15:578–81. [PubMed: 16537719]
31. McHale CM, Wiemels JL, Zhang L, et al. Prenatal origin of childhood acute myeloid leukemias harboring chromosomal rearrangements t(15;17) and inv(16). Blood 2003;101:4640–1. [PubMed: 12756163]
32. Wiemels JL, Kang M, Greaves M. Backtracking of leukaemic clones before birth . Methods in Molecular Medicine. 2008in press
33. Weisenberger DJ, Campan M, Long TI, et al. Analysis of repetitive element DNA methylation by MethyLight. Nucleic Acids Res 2005;33:6823–36. [PubMed: 16326863]
34. Liebich I, Bode J, Frisch M, Wingender E. S/MARt DB: a database on scaffold/matrix attached regions. Nucleic Acids Res 2002;30:372–4. [PubMed: 11752340]
35. Spitzner JR, Muller MT. A consensus sequence for cleavage by vertebrate DNA topoisomerase II. Nucleic Acids Res 1988;16:5533–56. [PubMed: 2838820]
36. Suzuki M, Savoysky E, Izuta S, Tatebe M, Okajima T, Yoshida S. RNA priming coupled with DNA synthesis on natural template by calf thymus DNA polymerase alpha-primase. Biochemistry 1993;32:12782–92. [PubMed: 7504526]
37. Selzer RR, Richmond TA, Pofahl NJ, et al. Analysis of chromosome breakpoints in neuroblastoma at sub-kilobase resolution using fine-tiling oligonucleotide array CGH. Genes Chromosomes Cancer 2005;44:305–19. [PubMed: 16075461]
38. Lewis SM, Agard E, Suh S, Czyzyk L. Cryptic signals and the fidelity of V(D)J joining. Mol Cell Biol 1997;17:3125–36. [PubMed: 9154811]
39. Thandla SP, Ploski JE, Raza-Egilmez SZ, et al. ETV6-AML1 translocation breakpoints cluster near a purine/pyrimidine repeat region in the ETV6 gene. Blood 1999;93:293–9. [PubMed: 9864173]
40. Pasqualucci L, Neumeister P, Goossens T, et al. Hypermutation of multiple proto-oncogenes in B-cell diffuse large-cell lymphomas. Nature 2001;412:341–6. [PubMed: 11460166]
41. Lee GS, Neiditch MB, Sinden RR, Roth DB. Targeted transposition by the V(D)J recombinase. Mol Cell Biol 2002;22:2068–77. [PubMed: 11884595]
42. Raghavan SC, Swanson PC, Wu X, Hsieh CL, Lieber MR. A non-B-DNA structure at the Bcl-2 major breakpoint region is cleaved by the RAG complex. Nature 2004;428:88–93. [PubMed: 14999286]
43. Lander ES, Linton LM, Birren B, et al. Initial sequencing and analysis of the human genome. Nature 2001;409:860–921. [PubMed: 11237011]
44. Yu F, Zingler N, Schumann G, Stratling WH. Methyl-CpG-binding protein 2 represses LINE-1 expression and retrotransposition but not Alu transcription. Nucleic Acids Res 2001;29:4493–501. [PubMed: 11691937]
45. Roman-Gomez J, Jimenez-Velasco A, Agirre X, et al. Promoter hypomethylation of the LINE-1 retrotransposable elements activates sense/antisense transcription and marks the progression of chronic myeloid leukemia. Oncogene 2005;24:7213–23. [PubMed: 16170379]
46. Gaudet F, Hodgson JG, Eden A, et al. Induction of tumors in mice by genomic hypomethylation. Science 2003;300:489–92. [PubMed: 12702876]

47. Ehrlich M. DNA methylation in cancer: too much, but also too little. Oncogene 2002;21:5400–13. [PubMed: 12154403]

48. Belgnaoui SM, Gosden RG, Semmes OJ, Haoudi A. Human LINE-1 retrotransposon induces DNA damage and apoptosis in cancer cells. Cancer Cell Int 2006;6:13. [PubMed: 16670018]

49. Gasior SL, Wakeman TP, Xu B, Deininger PL. The human LINE-1 retrotransposon creates DNA double-strand breaks. J Mol Biol 2006;357:1383–93. [PubMed: 16490214]

50. Rodriguez J, Vives L, Jorda M, et al. Genome-wide tracking of unmethylated DNA Alu repeats in normal and cancer cells. Nucleic Acids Res 2008;36:770–84. [PubMed: 18084025]

51. Zelent A, Greaves M, Enver T. Role of the TEL-AML1 fusion gene in the molecular pathogenesis of childhood acute lymphoblastic leukaemia. Oncogene 2004;23:4275–83. [PubMed: 15156184]

52. Bird A. DNA methylation patterns and epigenetic memory. Genes Dev 2002;16:6–21. [PubMed: 11782440]

53. Mutskov V, Felsenfeld G. Silencing of transgene transcription precedes methylation of promoter DNA and histone H3 lysine 9. Embo J 2004;23:138–49. [PubMed: 14685282]

54. Greaves M. Infection, immune responses and the aetiology of childhood leukaemia. Nat Rev Cancer 2006;6:193–203. [PubMed: 16467884]

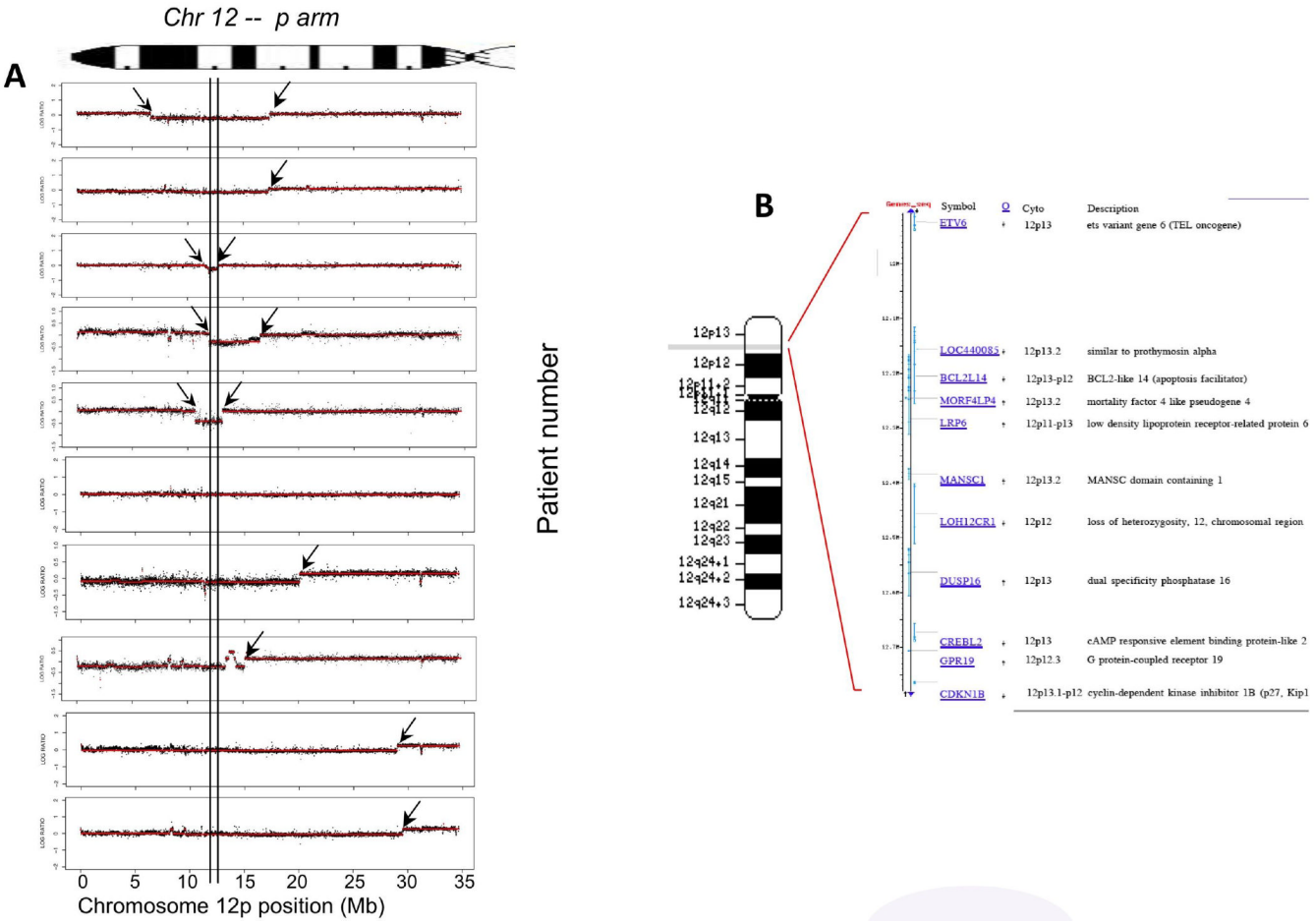


**Figure 1.**

***A***. Array comparative genomic hybridization of chromosome 12, p-arm. Isothermal tiling path array with 390,000 probes spaced at 50 bp intervals. $Log_2$ fluorescence ratios on Y-axis, tumor DNA (vertical up) *vs*. normal control (vertical down) on the Y-axis, the red line indicated the change point analysis. ***B***. Smallest commonly deleted region on chromosome 12 from the 10 patients displayed in Figure 1. The identities of the genes located within this region are indicated at the right.

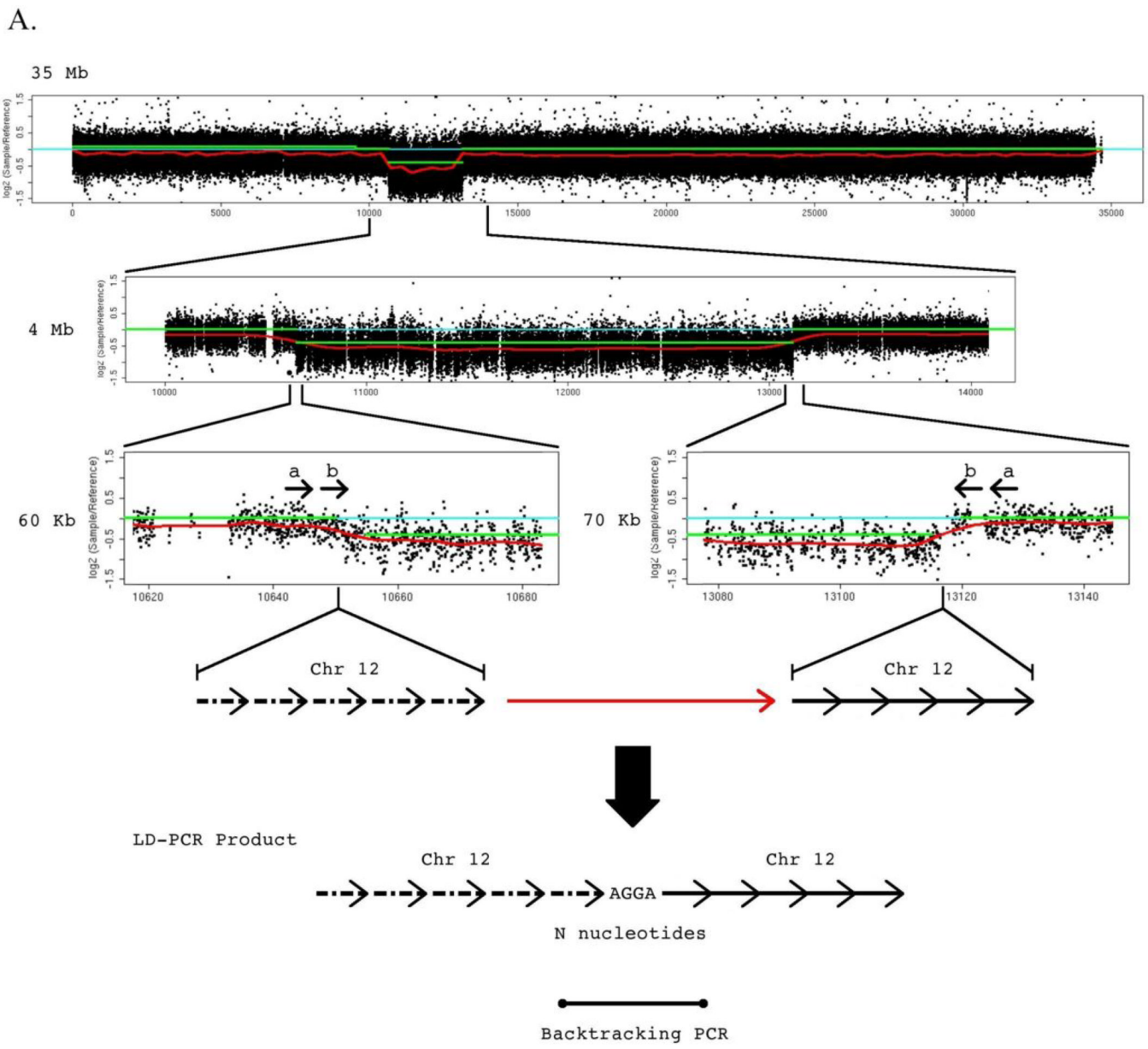

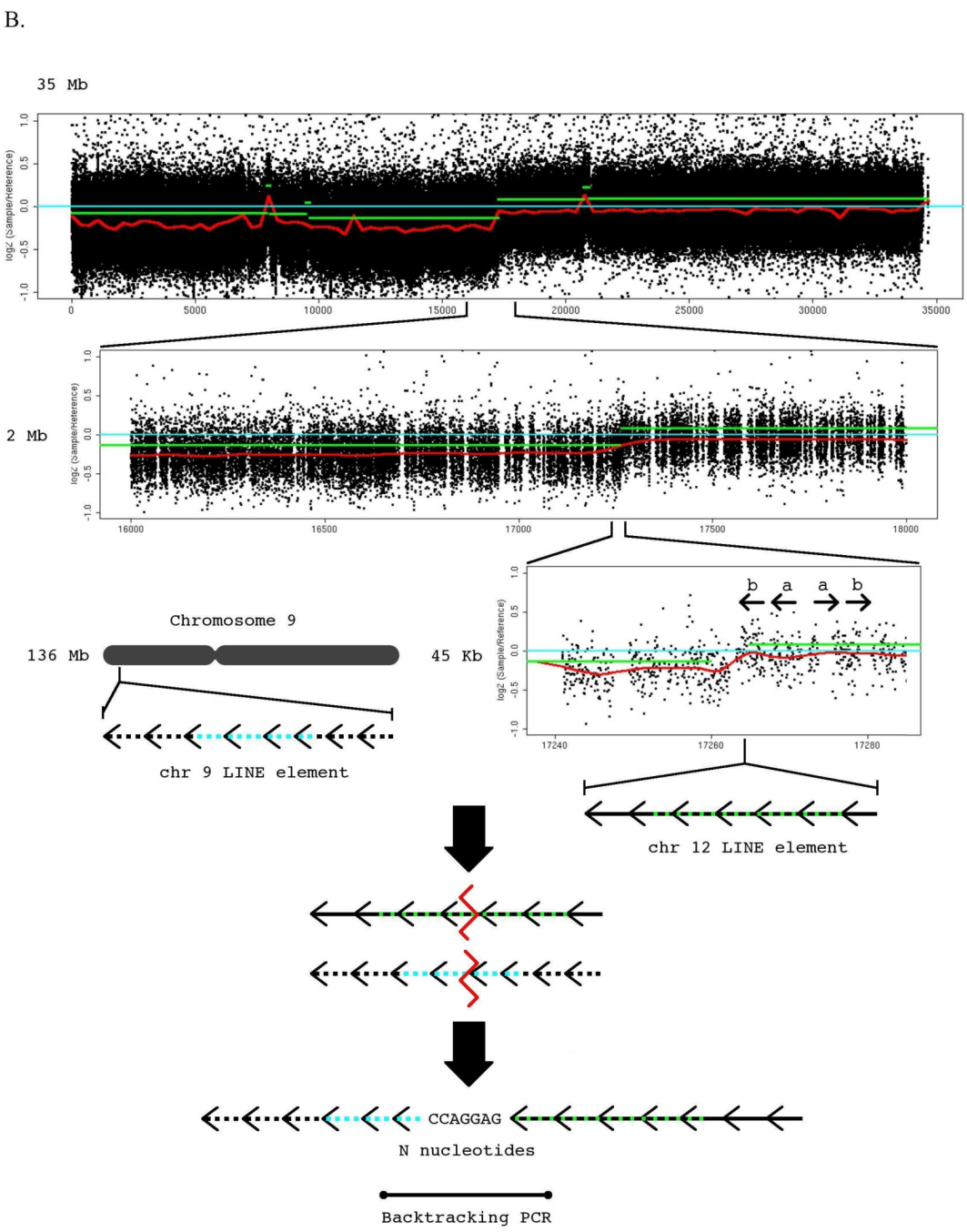


**Figure 2.**

Structure of del(12p) breakpoints and translocations. ***A*** and ***B*** indicate patients #5 and 2, respectively, as an example of an interstitial breakpoint (patient #5) and translocation (#2). X-axis scales of CGH plots are indicated at the left of each plot. The breakpoint is shown, with arrows indicating the direction of the sequence as numbered in human genome. Position of primers for sequencing the breakpoint (diagrammatically, not to scale) are shown — inverse primers for patient 2, and LD-PCR for patient #5. The first round primers are indicated with lower case “a” and the second round primers with lower case “b”. See Wiemels et al., (Ref #32) for more detailed methodology. Position of the backtracking PCR is noted at the bottom.

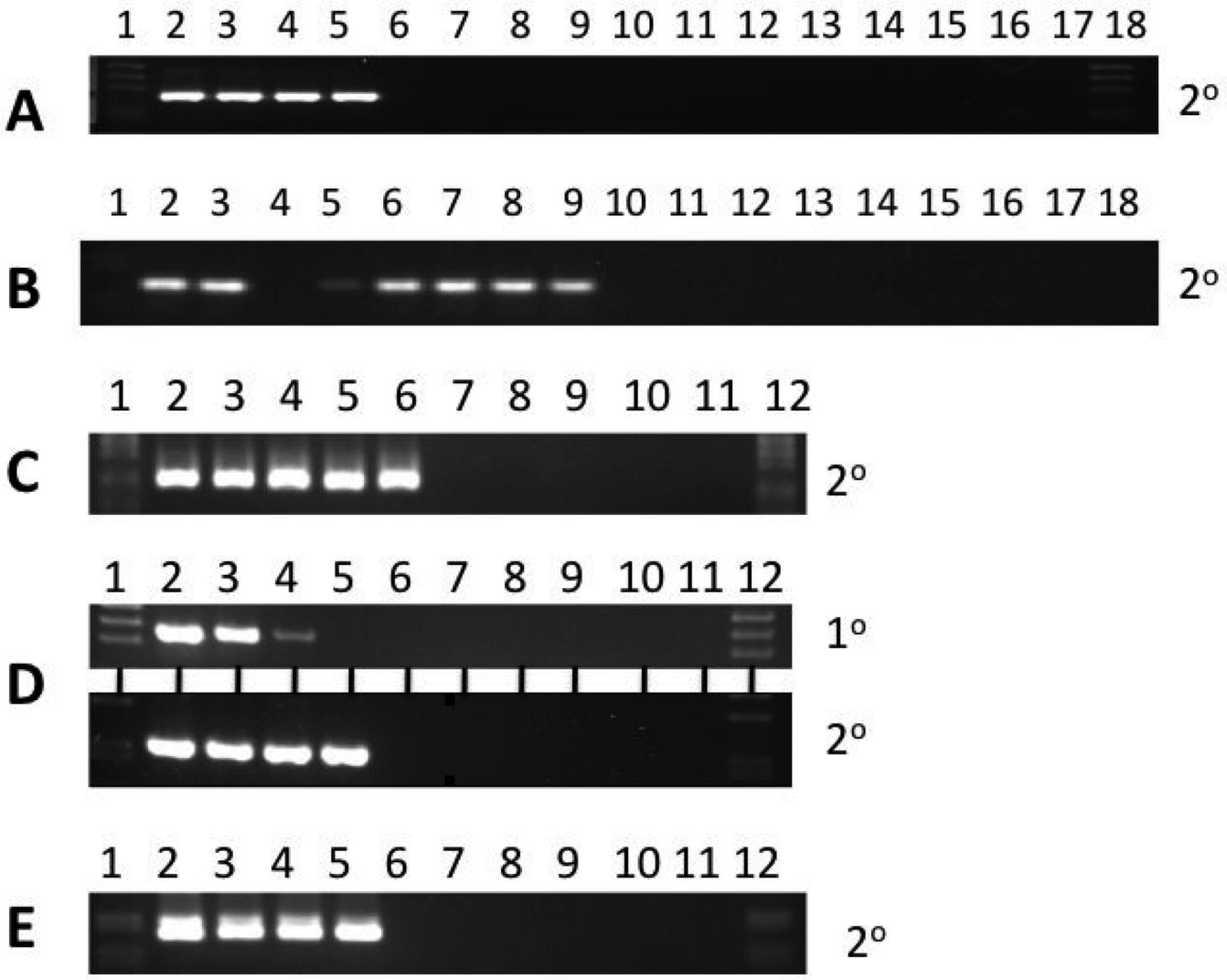


**Figure 3.**

Electrophoretic gels of backtracking del(12p) experiments in five patients as an example of results. ***A***. Secondary PCR for patient 1-F1 and 1-R1 primers. *Lane 1 & 18*, 1 kb ladder; *lane 2,3,4,5,6,7*: 100 to 0.001 ng patient 1 bone marrow serial dilution DNA; *lane 8, 9, 10 & 17*, blank; *lanes 11,12, 14*, and *15* various control lymphocyte DNAs from healthy NCCLS study control participants; and *lane 13 & 16*, 50 ng of patient #1 ANB card DNA. ***B***. Secondary PCR reaction for patient 5. Primers: patient 5-F1 and R1. *Lanes 1 & 18*, 1 kb ladder; *lane 2, 3, 5, 6, 7, 8, 9*: 100, 10, 1, 0.1, 0.01, and 0.001 ng patient 5 bone marrow DNA; *lanes 4, 10, 11*, blank; *lanes 12, 13, 15, and 16*, various control DNAs from healthy controls; and *lanes 14 & 17*, 50 ng of patient 5 ANB card DNA. ***C, D,*** *and* ***E***. patients #7, 8, and 10 respectively. *Lanes 2-7:* 100 to 0.001 ng patient 1 bone marrow serial dilution DNA in; *lane 7* blank; *lane 8 and 9*, DNA from healthy controls; *lane 10*, DNA from a control ANB card; and *lane 11*, 50 ng DNA from the interrogated patient's ANB card. In C, the primary PCR reaction is shown along with the secondary reaction. Gels ***A*** and ***B*** were performed by a different technician than gels ***C-E***.

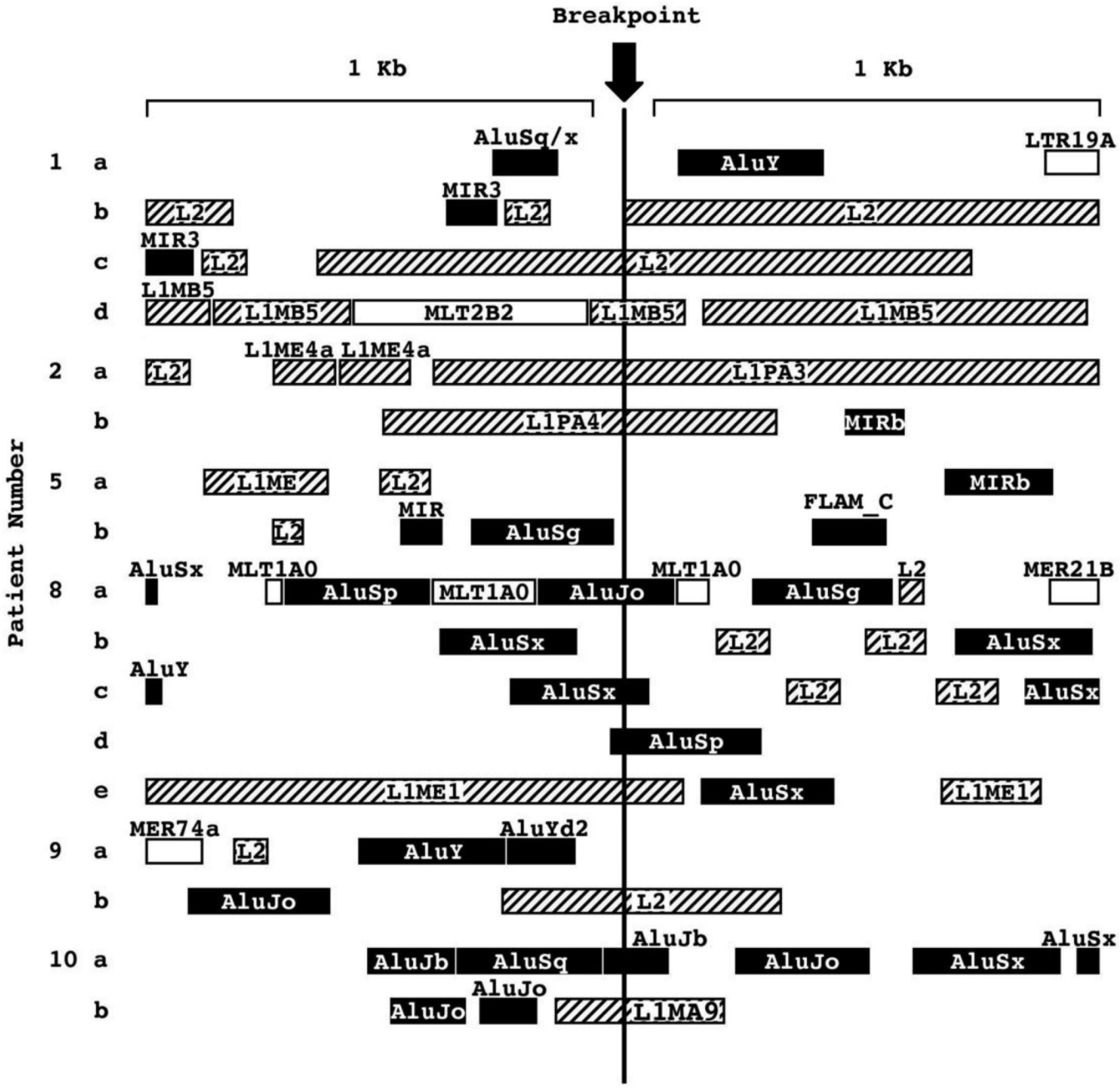


**Figure 4.**

Schematic representation showing the proximity and identity of repetitive elements in relation to the patient breakpoints. *Alu* sequences are in black, LINE elements in cross-hatched rectangles, and long terminal repeat sequences are open rectangles. The breakpoints are listed (a, b, c. . .) from left to right in relationship to the chromosome 12 arm (see Supplementary Table 2 for the data that this figure is based on).

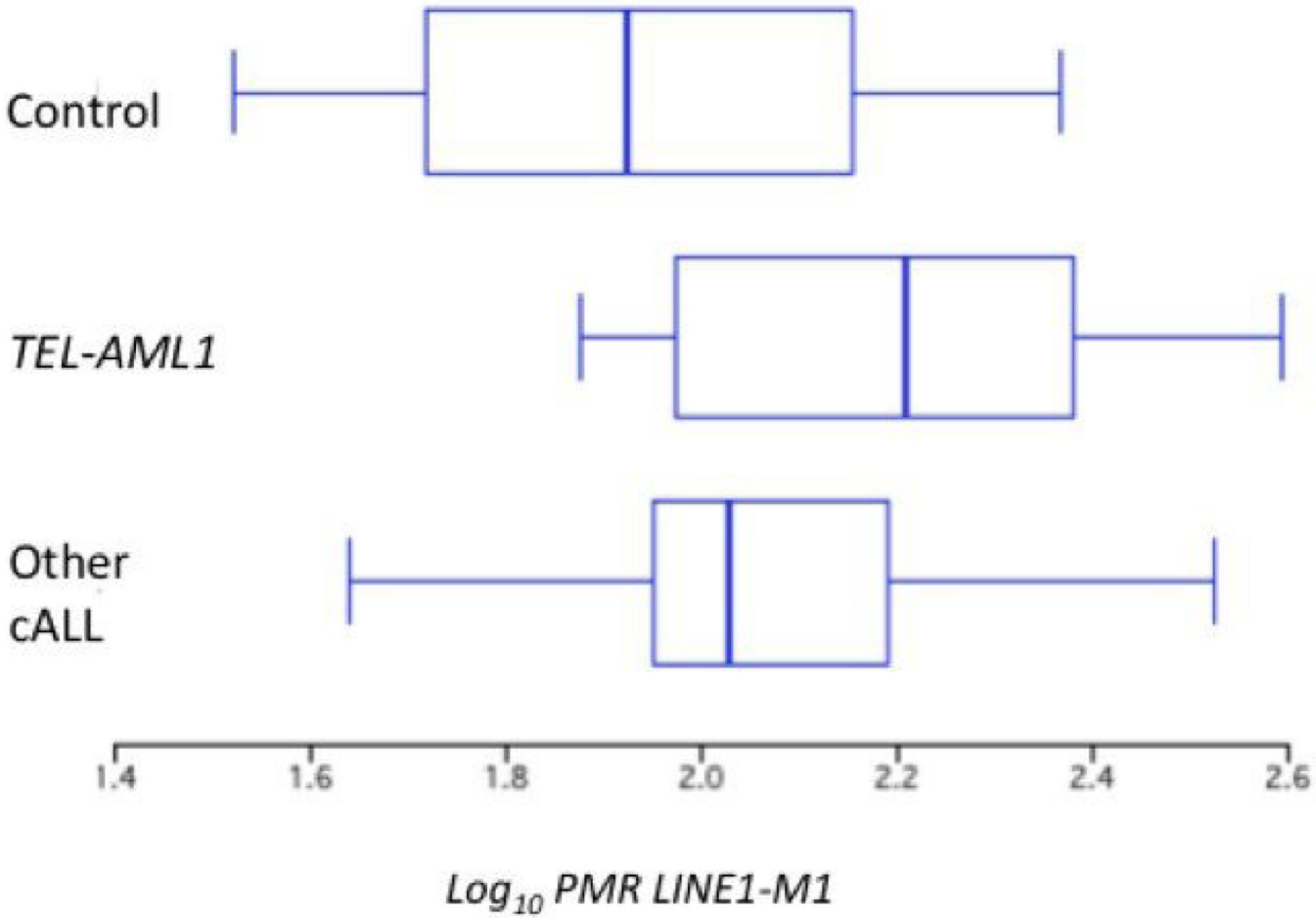


**Figure 5.**
LINE1-M1 methylation status in ANB cards from children who contracted leukemia later in their lives with *TEL-AML1* translocations, other cALL diagnoses, and who did not contract leukemia. The controls are age, gender, and ethnicity frequency-matched to cases. Data was $Log_{10}$ transformed to approximate normal distribution with the center box displaying two quartiles (bisected by the median) and the whiskers the marginal quartiles.

**Table 1**

Details of nine del(12p) breakpoints sequenced in six t(12;21)+ patients, and results of backtracking in archived newborn bloods.

| Patient | Age at Dx | Breakpoint Junctions* | | Genes on partners† | DNA aliquots tested‡ | Limit of sensitivity§ | Del(12p) Result‖ | TEL AML1 Result‖,†† |
|---|---|---|---|---|---|---|---|---|
| 1 | 3.1 | Chr2: 18566233 | Chr12: 17381863 | none none | 4 | 100 pg | Neg. | nt |
| | | Chr2: 18565559‡ | Chr4: 171899188‡‡ | none none | nt | nt | nt | na |
| 2 | 1.9 | Chr9: 4596202 | Chr12: 17262923 | C9orf68 none | 3 | 10 pg | Neg. | nt |
| 5 | 3.5 | Chr12: 10651543 | Chr12: 13116973 | MAGOH KIAA1467 | 4 | 10 pg | Neg. | Pos. |
| 8 | 6.7 | Chr12: 14332542 | Chr5: 15571213 | none FBXL7 | 2 | 100 pg | Neg. | Pos. |
| | | Chr5: 15571063‡ | Chr12: 13736983‡‡ | FBXL7 GRIN2B | nt | nt | nt | na |
| | | Chr12: 13735244 | Chr12: 15149854 | GRIN2B none | 2 | 100 pg | Neg. | na |
| 9 | 2.4 | Chr13: 30225531 | Chr12: 28980372 | ALOX5AP none | 3 | 100 pg | Neg. | Neg. |
| 10 | 3.1 | Chr19: 17983155 | Chr12: 29534763 | ARRDC2 OVCH1 | 2 | 10 pg | Neg. | Neg. |

*Breakpoint location on the indicated chromosome, using Human Genome vl8.

†Genes located at the breakpoint on the left, and right breakpoint, respectively. “None” indicates that the breakpoint was not within a gene; all genic breakpoints were located within introns and would not be predicted to form an “in frame” fusion gene in the cases where both partner breakpoints were located within genes (patients 5, 8, and 10).

‡The number of 50 ng aliquots of purified DNA from Guthrie cards.

§The lowest level of diagnostic DNA detectable in a two-round PCR reaction.

‖Neg - no presence of breakpoint DNA by PCR; Pos- positive presence of breakpoint sequence; nt - not tested due to limited DNA from Guthrie card, na - not applicable (only one *TEL-AML1* breakpoint per subject).

††Data from McHale et al., 2003.

‡‡Breakpoint not backtracked